



## The Effect of Secondary Flow on Droplets Behavior in Gas-Liquid Mixing Process Downstream of a Curved Duct

Abdulsattar J. Mohammed\*, Akeel A. Nazzal

Mechanical Engineering Dept., University of Technology-Iraq, Alsina'a street, 10066 Baghdad, Iraq.

\*Corresponding author Email: [asj\\_2006saraf@yahoo.com](mailto:asj_2006saraf@yahoo.com)

### HIGHLIGHTS

- Curved portion in inlet duct of gas turbine generators is a power boosting expedient.
- Secondary flow generated enhances the phase mixing due to momentum exchange.
- Wider bend angle promotes mass and heat transfer rates within four cell vortices.
- Mixing process is greatly sensitive to flow within the inner half of a curved duct.

### ABSTRACT

Experimental and numerical investigations are carried out on water injection in a humidification process of air traveling steadily through the curved part with a constant cross-section. A principal aim is to study the flow behavior through the curved duct and the generation of secondary flow. The effect of bend angle on the development of secondary flow and flow structure intensities and enhancement of the heat and mass transfer downstream the curved duct. Moreover, the influence of the mixing process between liquid and gas in an air humidification process was examined. Experiments were performed with an average air velocity range from (2.5 to 5 m/s) while keeping the water injection rate of (19 kg/h) through (50) cm square wind tunnel includes three bend angles of (45°, 90° and 135°) along with three sets of nozzle tilt angles of (-45°, 0° and 45°) to the axial flow direction. The study also implies a numerical analysis using ANSYS FLUENT 2019 R3 with the turbulent model of RNG using (k-ε). Experimental results showed that the optimum operating condition (greater extent of cooling and humidification) was obtained with a bend angle of 135° at axial water injection, i.e., 0° nozzle tilt angle at the lowest air velocity of 2.5 m/s. This could be attributed to the strong identical vortices developed and better droplet distribution across the duct, and more time available for heat exchange between water droplets and the air stream. The maximum reduction in treated air temperature was 28 %, with 219% in the relative humidity of the air stream. This condition gave corresponding cooling effectiveness of 58%.

### ARTICLE INFO

**Handling editor:** Muhsin J. Jweeg

**Keywords:**

Curved duct  
Bend angle  
Flow structure  
(PIVLAB) Technique  
Fluid mixing

### 1. Introduction

Fluid flow in curved ducts has been studied for a long time due to fundamental engineering and industrial applications. It is essential for industrial equipment design, especially in air conditioning and fluid processing methods and several other equipment types. One of the essential things in this part is the bend angle or change in airflow direction because it affects the form of flow and distribution. The bend angle in the flow network leads to losses on the flow. In contrast, the duct network has many different sizes of bend angles. In addition to essential aspects, things are "the formation of secondary flow pattern in the duct cross-section area resulting from the imbalance developed between the centrifugal force and the radial pressure fields". Also, the different values of fluid velocity between the near part of the surface to the middle part, resulting from the generation of the boundary layer near the duct's surface, causes the generation of vortices inside the flow.

The secondary flow negatively affected fluid movement in specific applications because it leads to losses in the flow. Nevertheless, it is possible to employ this flow form in many applications because secondary flow enhances the friction factors and heat and mass transfer rates over their straight-duct values. Many researchers investigated the effect of secondary flow on heat transfer in bend ducts. Three-dimensional numerical investigation was simulating the secondary flow development with curvature ratio of ( $\delta=15.1$ ) curvature ratio of a square curved duct for Newtonian viscous flows to conduct the effect of Dean number on the flow structure including three Dean number of ( $Dn=125, 135, 150$ ). The study showed that the swirls are strongly correlated with Dean number change, evident through the size and number of vortices generated, which observe only a pair of vortices generated at  $Dn=125$  because of the weak effect of the centrifugal force on the flow. However, when increasing Dean's number to  $Dn=135$ , additional other pairs of small vortices appear at the bend angle (90°). For the high value

of Dean number, i.e.,  $Dn$  equal to more than 160, the centrifugal forces motivate the appearance of other pair started at  $(\theta=85^\circ)$  [1]. Investigate experimentally and numerically the flow structure, and turbulence intensity inside the duct with three different curvature ratios for the same curved duct (0.25, 0.5, 0.75) at average airstream velocity remain constant at 5m/s all testing cases. The PIV images "indicate a Pair of Dean vortices generated for all curvature ratios, with the inner side vortices moved outward when decreasing the curvature ratio as a result of centrifugal effect flow separation". The numerical analysis showed that the slight mixing influences the swirl intensity due to changing Reynolds number, and it is more affected by the change of curvature ratio[2]. Conducted an experimental study on the turbulent flow through a smooth wall pipe with  $(90^\circ)$  bend has a curvature ratio  $(\delta=1.5)$ . The technique used is the hot wire of a rotating probe with an inclined wire. Results show that the presence of a pair of vortices due to the acceleration of the primary flow near the inner wall, which led to the generation of secondary flow moving from the outer to the inner wall of the bend, occurs in the bend and remains even at  $L/D=10$  [3]. The numerical investigation by [4] of the effect of bend pipe angle on the velocity and pressure drop and study behaviors of fluid flow through pipes. In this study, we have taken different bend pipes of different angles (a)  $90^\circ$  bend pipe (b) Greater  $90^\circ$  bend pipe (c) Less  $90^\circ$  bend pipe with constant decimation of the other part of the pipe (diameter and length). The case assumption that was fully developed flow, Steady, and laminar flow was using ANSYS FLUENT to solved The continuity equation and Navier-Stokes equations. The working fluid in this study is Water vapor. The results show a change of the pressure and velocity distributions in different bend pipes for the same boundary conditions. The magnitude of velocity and pressure drop of less  $90^\circ$  bend pipe is greater than the  $90^\circ$  and greater  $90^\circ$  bend pipe. Less  $90^\circ$  bend pipe case has the highest pressure in the inlet region compared to other cases due to the bend angle of the pipe. For this reason, we can say that less  $90^\circ$  bend pipe is more beneficial to convey fluid than the  $90^\circ$  and greater  $90^\circ$  bend pipes. The present findings may help understand the bend pipes' flow behavior at any pumping stations or water refineries. Conduct an experimental investigation of the curvature ratio when exposed to the fully turbulent flow in the tube. The Reynolds number was  $(5 \times 10^4)$ , and the curvature ratio was  $(\delta=6)$ . They used hotwire techniques to measure the three velocity components and six components of the Reynolds stress along a horizontal and regular plane through the stream-wise places for different rejoin ranges from 18 D upstream of the curve duct to 18 D downstream the curved duct of U shape. The numerical results of the study presented that the secondary flow was recognized at the curvature driven by the centrifugal force and is inveterate by numerical simulation modeling of flow pattern using the  $(k-\epsilon)$  model. Proof of a second vortex cell is obtained within the curvature, and it is verified again through the numerical results and previous total pressure measurements [5]. Perform an experimental and numerical analysis on the curved pipe turbulent airflow. A curved pipe was used with an inner diameter of (4.3 cm) and had two curvature ratios (13.95, 6.98) to determine the bending effect on the flow. The corresponding Dean numbers were respectively (9138 and 12919), and the number of Reynolds for both cases was (34132). The experimental aspect was based on the laser Doppler anemometry (LDA) to measure the RMS (Root mean square) and the mean stream-wise velocities. The numerical modeling aspect was based on the computer package employing  $(k-\epsilon)$  turbulence model. The results showed that the secondary flow was more prevalent at the smaller bend, and an encouraging agreement was obtained between the numerical and experimental results[6]. Investigate the Incompressible single-phase turbulent flow numerically through a circular section of  $(90^\circ)$  pipe bend using  $(k-\omega)$  standard model. The study included two bends with the diameter  $(D=0.104 \text{ m})$  and curvature to diameter ratio  $(R_c/D=2 \text{ and } 1)$  with the same inlet velocity  $(U_{in}=8.7 \text{ m/s})$  of working fluid (air) have been used for the study. The velocity fields of the primary and secondary flows and the Turbulent Intensity distributions in different sections have been illustrated. Numerical results show that flow separation can be visualized for bend with a strong curvature. Distributions of the velocity vector show that the secondary flow induced by the movement of fluid from the inner to the outer wall of the bend leading to flow separation; in the case of  $R_c/D=2$ , no separation occurs while in the strong curvature case of  $R_c/D=1$ , a separating flow appears along with the inner core[7]. Experimentally investigated secondary flow developing fields in the entrance section of a rotating straight channel using Particle Image Velocimetry (PIV). Reynolds number and rotation number on the development of the secondary and the effects of stream-wise position. The increase of the Reynolds number was found to induce the merging position to move upstream. The secondary flow development along with the stream-wise direction results from the movement, generation, and vanishing of the vortex lines [8]. Humidification is a fundamental process in many applications, such as air-conditioning systems that aim to deliver air at the required conditions to achieve human comfort. The humidification process is meant to produce a fine spray of liquid in a gaseous environment. A spray is a collection of moving droplets moving in a controlled shape and direction. The smaller diameter of the liquid droplets, the high rate of evaporation is done due to the tremendous interfacial area between the liquid and gas. When air flows through an atomized water spray, an increase in the humidity ratio and a drop in the air temperature because of the latent heat absorption from the flowing air as mentioned by [9], the generation of smaller diameter droplets increases the contact area between spray of water droplets and airstream, thus producing more evaporation cooling rate and. The systems of sprays are similarly of primary importance in influencing the form and penetration of the resultant spray, as described by [10]. The Evaporative cooling process is a quick and efficient way to cool hot and dry air. Even though it provides a low-cost, energy-efficient solution, environmentally friendly (not causing ozone-damaging by the used CFC compounds) compare to an alternative method to inlet air cooling [11].

There are two main strategies to obtain direct evaporative air cooling based on the contact method between the air stream and water droplets. The first technique brings the air and water in direct contact with each other using a wetted honeycomb as a wetted media to ensure good contact. In contrast, the air is forced through the wetted media using a different types of fans. However, this technique ensures good contact, but the percentage of evaporative cooling effectiveness, is not more than (90-95) %, while the second evaporative cooling method is obtained by evaporating too fine water droplets sprayed (fogging system). Perform an experimental investigation to conduct the effect of atomizer position within a curved duct on the evaporative cooling process. A square duct with (50 cm) side was used. At the same time, The air velocity in the main test

section was (14m/s) with Reynolds number ( $Re=4.16 \times 10^5$ ) according to the calculations carried out corresponding to technical information attached to the gas turbine unit (V94.3a) installed at Kirkuk gas turbine power plant. However, the water flow rate of (0.24 ml/s) to spray on the airstream and the ambient temperature (43°C). The results showed that the relative humidity decreases by increasing the ambient air temperature, leading to a higher air stream ability to contain water vapor. It was evident that increasing the water atomization from rate (7 to 24.2) ml/s leads to an increase in the relative humidity from (14.7%) to (44.2%) at 24.2ml/s, besides temperature drop of cooling (17°C) occurs at the higher water atomization rate of 24.2ml/s. At the same time, it was only (9.6°C) at 7ml/s[12]. Experimental investigated the effect of turbulences on a gas-liquid mixing process downstream of a curved duct using water injection into airflow inside the curved duct. The experiments were conducted on wind tunnels with dimensions of (50×50 cm) at air average velocity (10 m/s). The air to water ratio ranges between (1000 and 2000), and the ambient temperature range from (30° to 50°C). The result shows that the best performance of the water injection system was obtained at the central position of (25 cm) with ( $\Phi=0^\circ$ ). The maximum temperature reduction is (26%) and the relative humidity is increased by the ratio of (2.13) at a higher environmental temperature of (45.2°C) and a flow ratio of (1000) [13]. Experimental and numerical investigation of the influence of curvature ratio on mixing process of evaporative cooling of stream air by using water injector and studying the nozzle matrix fixed position upstream of a bent duct. The investigation relies on three different curvatures ratio of the duct range from (0.25, 0.75). The nozzles design and configuration of the matrix are accomplished conferring to the result of flow structure from simulation using analysis with the turbulent model RNG-k- $\epsilon$ . The numerical results demonstrate that the best curvature ratio is 0.75, which gives the best humidification system and performance, which leads to 53.63%, relative humidity increase, and 17% temperature reduction. However, the optimal nozzle location was 3  $D_H$  upstream of the bend [14]. The gas turbine's power output and fuel consumption strongly depend on the mass flow rate, quality, and ambient temperature of the air inducted into the unit. Therefore, a need to boost the gas turbine power output during the peak load periods during hot summer is required. The high temperature causes the air density to decrease, reducing the mass flow of compressor intake air.

## 2. Aim of the present work

The present work explores secondary flow patterns through the simulations Fluent to study different bend ducts and Reynolds's number effect on the flow structure generated. The improvement of fluids mixing downstream the bend is to be decided according to the best bend angle that achieves the better humidification of the air stream in a practical situation such as the inlet ducting of a gas turbine generating unit aiming to moisten the air and reduce its temperature in the purpose of enhancing the power output during hot summer climates. The geometry of the bend is greatly influenced the flow field and the rates of heat and mass transfer. This study is motivated to investigate both experimentally and numerically the effect of changing bend angle on the evaporative cooling of steady turbulent airflow through the square duct. It is considered a simulation of the fogging process applied to the compressor inlet air in a gas turbine engine aiming the boost power output.

## 3. Experimental Setup

The test rig used in this study is mainly a subsonic wind tunnel having a square cross-section with (50 cm) sides. The layout of the wind tunnel schematically is displayed in Fig. 1. The air enters the wind tunnel through a bell-mouth-shaped duct that purposes to "decrease the effects of inlet turbulence and produce steadily flowing air". The bell mouth is connected to the first (3 m) straight duct to accommodate inlet air preheaters and humidifiers. The bent portion is connected to the end of the first straight duct to generate the secondary flow needed to mix the injected water with the air stream. In the present work, three bent ducts were used with a bend angle of (45°, 90°, and 135°) as shown schematically in Fig. 2. These bend angles are chosen according to the regulations of ASHRAE (2000)[15]. The downstream end of the bent duct is connected to another (3 m) straight duct leading the air to the axial fan running at (1500 RPM) responsible for the induction of air through the wind tunnel. The airflow is adjusted by double butterfly gates built into the fan outlet. The air means velocity at fully opened gates (5 m/s) ( $Re = 1.43 \times 10^5$ ). The air inlet condition is kept fixed throughout all tests at (45 °C) dry bulb temperature and (15%) relative humidity. The air temperature is adjusted using eight electric preheaters with a total capacity of (24.5 kW). The heater is shown in Fig. 3-A. On the other hand, a steam humidifier is used to fix the air's relative humidity, leaving the heaters to the desired value (15%). The steam humidifier consists of two heaters with a total capacity of (15 KW) arranged in two steps. The steam is brought toward the wind tunnel by a steam distributor, as shown in Fig. 3-B. The humid air properties are measured using a DHT22 ARDUINO system containing 25 DHTD22 sensors measuring the humidity and temperature at the main test section installed at the fan entrance. The ARDUINO system data are sent to a PC to be saved and analyzed, as shown in Fig. 4 A and B. There are also four sensors installed after the air treatment system to ensure that the simulated ambient condition is at the desired values. The nozzles matrix contains nine nozzles with 0.1mm diameter nozzles placed in the first straight duct with the ability to be moved axially in advance to the bent duct inlet. The matrix is connected to the fog machine supplying water under a pressure of (70 bar), as shown in Figs. 5 and 6. The nozzles can rotate from (-90° to 90°) with the axial flow direction. The water flow rate was measured by Rotameter-1100. Measuring the air velocity is done using a standard elliptical nosed Pitot-static tube installed in the first straight duct.

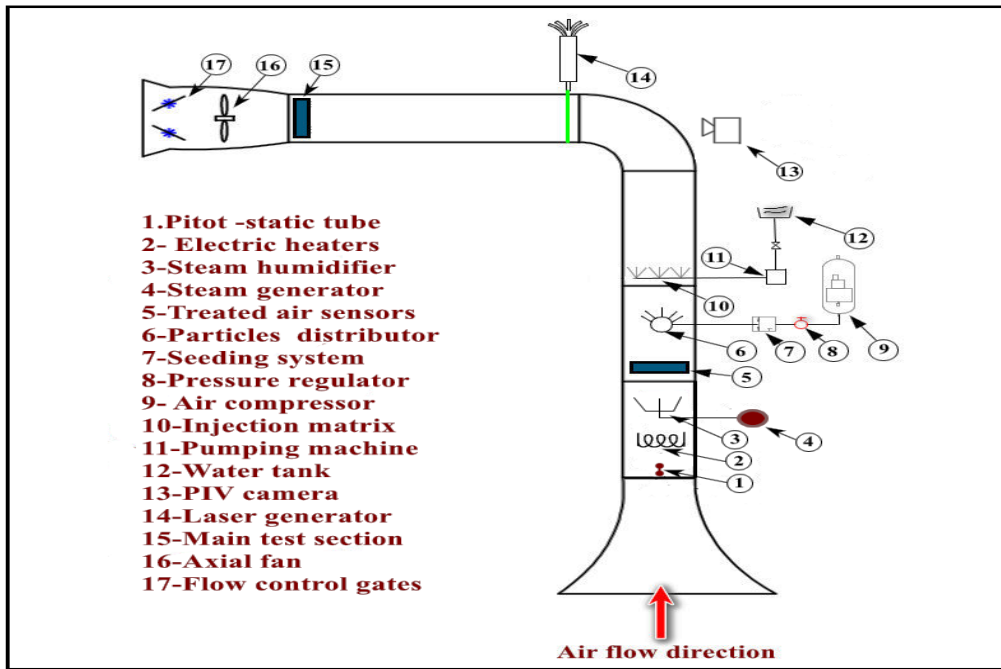


Figure 1: Schematic diagram of the test rig showing details of installed equipment

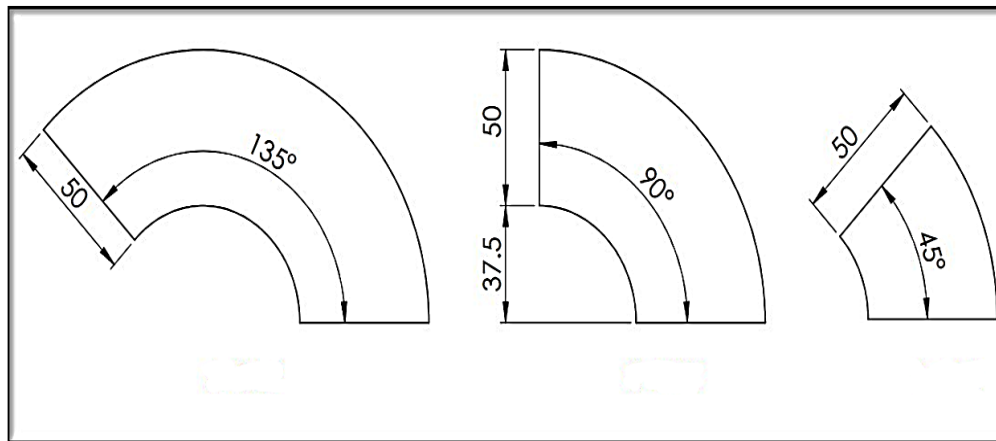


Figure 2: Three bent ducts with different bend angles at a curvature ratio of 0.75

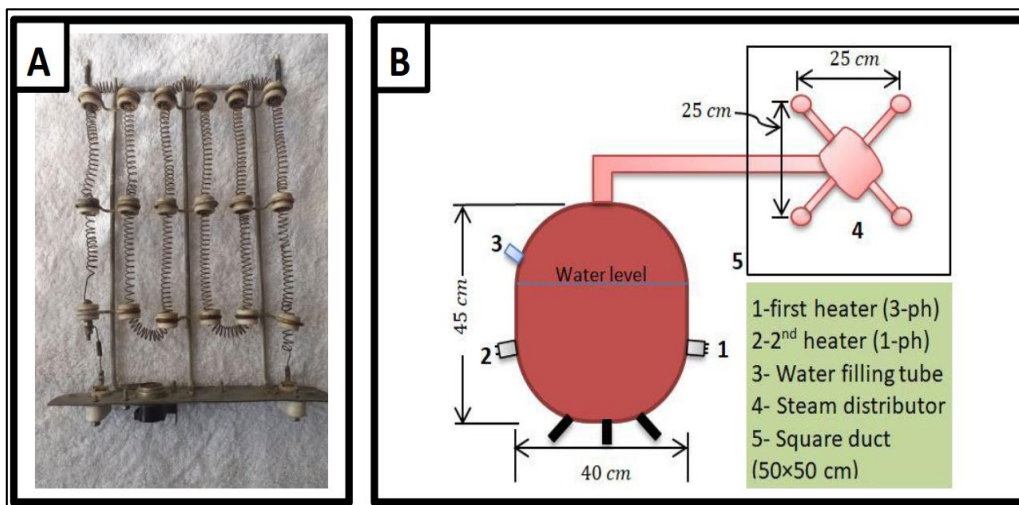


Figure 3: (A) Air beater; (B) Steam generation systems

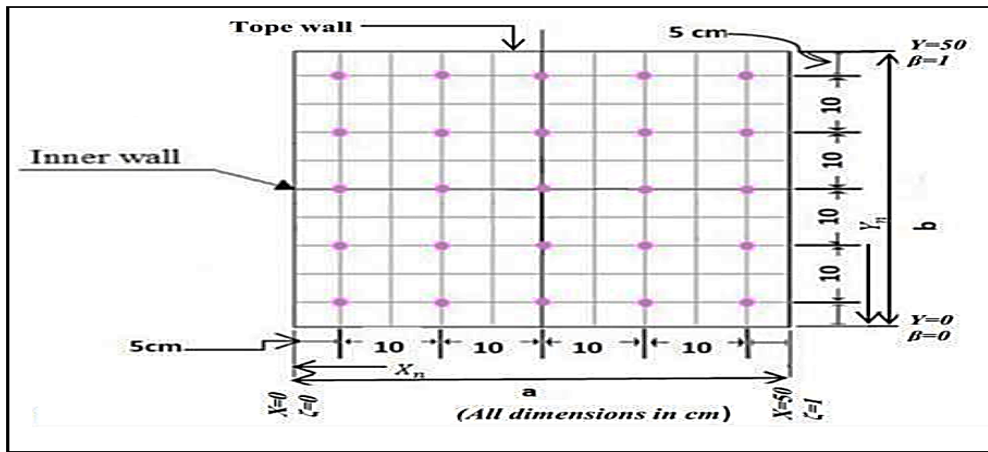


Figure 4: ARDUINO sensors linked to data acquisition system on PC

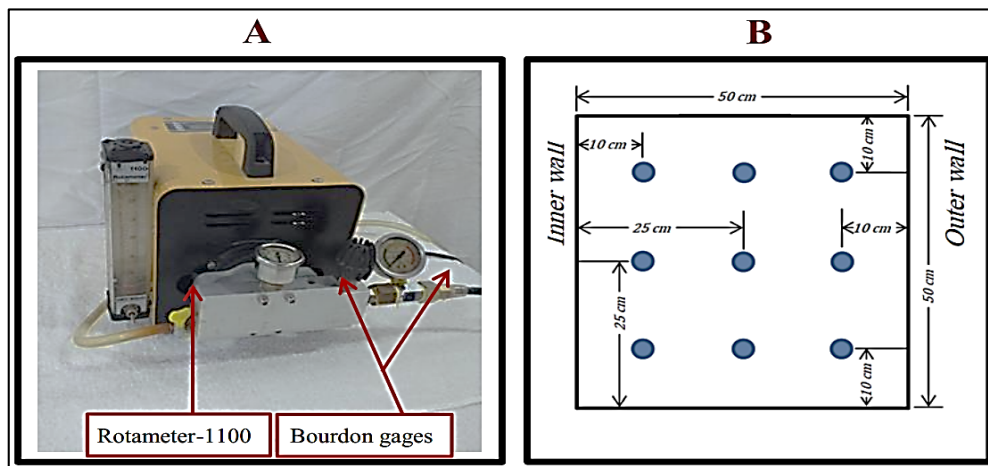


Figure 5: (A) Rotameter-1100 and Bulb Water Flow; (B) The nozzles matrix distances

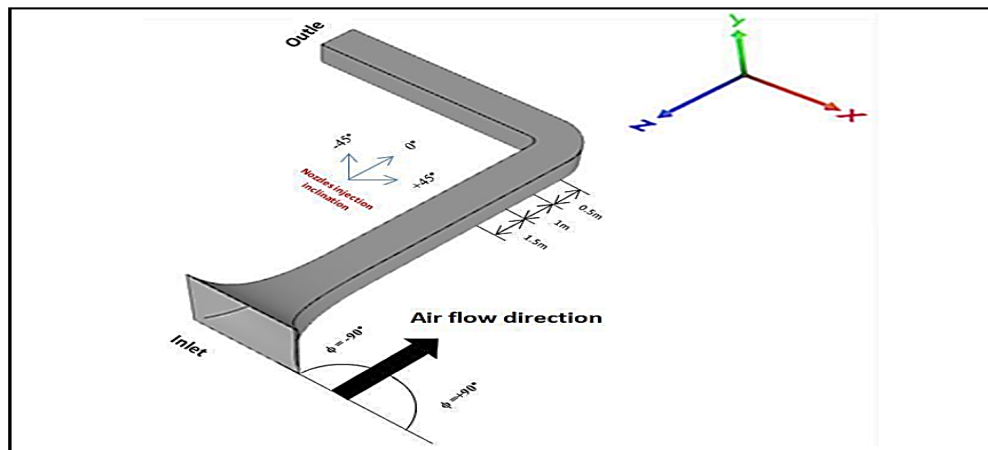


Figure 6: Coordinate system of the test rig showing the orientation of water injection

### 4. Numerical simulation

The governing differential equations fluid flow and heat transfer conservation of mass, momentum, and energy are presented. The computational fluid dynamic (CFD) is one of the most valuable tools for complex phenomena without resorting to expensive prototypes and difficult experimental measurements. Computational Fluid Dynamics (CFD) is a technique, which uses numerical analysis and data structures to solve two-phase flow problems. CFD analysis gives a deep understanding of the process mechanisms and shows the source of the problem. Analysis steps for FLUENT software package were used to develop the CFD model of cooling a hot air stream by water injection using species transport and discrete phase models of ANSYS FLUENT2019 R3 CFD simulations used FLUENT software with solver strategy to create the geometry and grid and solving simulations equations. As listed in Table (1), three air velocities were used, which are chosen to study the effect of changing Reynold number, bending angle, and the nozzles tilt angle on the flow structure and mixing process.

#### 4.1 Physical model

The following practical assumptions of the physical model were assumed to carry out the CFD simulations using ANSYS FLUENT program:

- Steady-state
- Turbulent flow.
- Newtonian fluid.
- Incompressible.
- Three-dimensional.
- The air continuous flow is treated as a single-phase homogeneous.
- Water is treated as a discrete phase flow.

#### 4.2 Turbulence Model

The models used in FLUENT, depending on the average time with modified equations, include unknown variables. To determine these variables in known quantities, turbulence models are needed. The considerations for turbulence model choice depend on the physical properties included in the flow, the used practice for a specific type of problem, the requirement of accuracy, computational resources, and simulation time [16][17]. The standard model of k-ε is used in this study. The turbulence kinetic energy  $k_f$  and its rate of dissipation  $\varepsilon_f$  Obtained from the following transport equations based on [18], [19].

$$\frac{\partial}{\partial t}(\rho_f k_f) + \frac{\partial}{\partial x_j}(\rho_f k_f U_{fi}) = \frac{\partial}{\partial x_j} \left[ (\alpha_k \mu_{eff}) \frac{\partial k_f}{\partial x_j} \right] + G_k + G_b - \rho_f \varepsilon_f - Y_M + S_k \quad (1)$$

And

$$\frac{\partial}{\partial t}(\rho_f \varepsilon_f) + \frac{\partial}{\partial x_j}(\rho_f \varepsilon_f U_{fi}) = \frac{\partial}{\partial x_j} \left[ (\alpha_{\varepsilon_f} \mu_{eff}) \frac{\partial \varepsilon_f}{\partial x_j} \right] + C_{1\varepsilon_f} \frac{\varepsilon}{k_f} (G_k + G_{3\varepsilon} G_b) - C_{2\varepsilon_f} \rho_f \frac{\varepsilon_f^2}{k_f} + S_{\varepsilon_f} \quad (2)$$

**Table 1:** List of flow conditions investigated in the current study, at Td=45 °C, RH=15%

Test No.	U <sub>ava</sub> (m/s)	Reynolds number	Bend angle λ	Investigated
Run 1	5	14.3×10 <sup>4</sup>	45°	Experimental
Run 2	3.75	10.73×10 <sup>4</sup>		+
Run 3	2.5	7.15×10 <sup>4</sup>		Numerical
Run 4	5	14.3×10 <sup>4</sup>	90°	Experimental
Run 5	3.75	10.73×10 <sup>4</sup>		+
Run 6	2.5	7.15×10 <sup>4</sup>		Numerical
Run 7	5	14.3×10 <sup>4</sup>	135°	Experimental
Run 8	3.75	10.73×10 <sup>4</sup>		+
Run 9	2.5	7.15×10 <sup>4</sup>		Numerical

#### 4.3 Performance Criteria in Humidification Process

Like any psychrometric process, air humidification complies with the same criteria usually commonly used in psychometrics. This paragraph is dedicated to judging the inlet air treatment by humidification via exploring the experiment results in this context.

#### 4.4 The Cooling Effectiveness

Any heat transfer process can be evaluated via the use of the effectiveness concept. The effectiveness essentially compares the attainable temperature drop with that available for utilization, which is the process potential. The effectiveness is given by;

$$\varepsilon = \frac{t_{db,i} - t_{db,o}}{t_{db,i} - t_{wb,i}} \quad (3)$$

Where

ε= direct evaporative cooling or saturation effectiveness, %

t<sub>db,i</sub>= dry-bulb temperature of entering air, °C

t<sub>db,o</sub>= Average dry-bulb temperature of leaving air, °C

t<sub>wb,i</sub>= wet-bulb temperature of entering air, °C

### 5. Results and discussion

The secondary flow is the critical element of a curved open-channel flow; a detailed analysis of the secondary flow structure is essential. This section investigates the secondary flow features with a focus on their development along different bend ducts. Three air velocities were used, which are chosen to study the effect of changing Reynold number, bending angle,

and nozzles tilt angle on the flow structure and mixing process. The flow conditions were investigated to study the flow structure showing different secondary flow shapes (rotating vortices) depending on the bend angle and airflow rate. Figure (7) (A, B, and C) show flow structure downstream for different curve bend angles and air velocities. In the case of bend angle ( $\lambda=45^\circ$ ), it was found that a pair of vortices are generated as a result of the high centrifugal forces and changing the fluid velocity and direction, while the study of flow structure in the second case of bend angle, i.e. ( $\lambda=90^\circ$ ) showing a generation of two pairs of vortices, one big near the inside of the duct and a small one near the outside of the duct, nevertheless the third case of bend angle ( $\lambda=135^\circ$ ) showing two pairs of vortices. At ( $\lambda = 45^\circ$ ), the flow keeps a two-vortex structure until downstream the curved part of the duct for all three air velocities. Because the centrifugal forces are not large enough to generate more vortices, the two-vortex flow structure remains intact; this result agrees with M. Boutabaa et al. [1]. Nevertheless, at ( $\lambda = 90^\circ$ ), viscous effects can no longer retain the two large vortex structures, and small pair near the outside of the duct appears. However, the growth rate of the other vortices is faster at ( $\lambda = 135^\circ$ ) than the other bend duct because the centrifugal forces are even leading to the development of the four-cell pattern observed down to the curved duct exit. Also, remark that the strength and size of the small vortex pair at the bend angle of ( $90^\circ, 135^\circ$ ) depend on the air velocity. It found that close to the outer wall of the duct in the case of low velocity (2.5 m/s) and become sharper and begin to shift towards the middle whenever the velocity of flow increases; this behavior is due to the increase Dean vortices. Further increase in ( $De$ ) causes an increase in centrifugal force leading to the development of additional regions of pressure gradient near the outer wall of the duct, and this result is in agreement with N. Nivedita et al. [20] From the observation of Figure (8) and (9) (A, B, and C), it found that the velocity (2.5 m/s) presents the most significant decrease in the temperature as the amount of temperature reduction is (52.58%) at the nozzles tilt angle ( $\phi= 0^\circ$ ) compared to the air velocity (5 m/s) because lower velocity provides a longer time for the heat exchange between Water droplets and airstream. The improvement in the relative humidity of air for changing the velocity from (5 to 2.5 m/s) is about (64.85%) due to the increased evaporation of water droplets for the bend angle ( $\lambda=45^\circ$ ). while for the second case bend angle of ( $\lambda=90^\circ$ ) the temperature reduction is (44.92%) corresponding to the relative humidity improvement (54.90%) at the nozzles tilt angle ( $\phi= 0^\circ$ ). Nevertheless, for the third case of bend angle ( $\lambda=135^\circ$ ), the temperature as the amount of temperature reduction is (43.39%) corresponding to the relative humidity improvement of about (54.02%) at the nozzles tilt angle ( $\phi= 0^\circ$ ). Figure (10) (A, B, and C) shows the effectiveness of evaporative cooling of humidified air streams at different air velocities and different nozzles tilt angles adopted in the current study. It is also evident from the figure that velocity (2.5 m/s) provides the most significant improvement in the evaporative cooling process than other velocities due to increasing the heat exchange duration between water droplets and airstream. According to the figure for the bend angle ( $\lambda=45^\circ$ ), at the velocity of (2.5 m/s), the achieved effectiveness was (46.65, 42.21, 33.77%) for corresponding tilt angles of ( $0^\circ, -45^\circ, +45^\circ$ ). Nevertheless, for the velocity of (5 m/s), the effectiveness only reaches a value of (22.12, 21.33, 16.38%) for the same respective tilt angles. While From the figure at a velocity of (2.5 m/s) for the bend angle ( $\lambda=90^\circ$ ), the effectiveness was (51.26, 50.32, 38.88%) for corresponding tilt angles of ( $0^\circ, -45^\circ, +45^\circ$ ). Nevertheless, for the velocity of (5 m/s), the effectiveness only reaches a value of (28.23, 27.44, 22.32%) for the same respective tilt angles. Nevertheless, the case of bend angle ( $\lambda=135^\circ$ ) gives the best cooling and humidification compared to the other bend angle which at the velocity of (2.5 m/s), the effectiveness attained was (57.97, 53.1, 47.01 %) for corresponding tilt angles of ( $0^\circ, -45^\circ, +45^\circ$ ). However, for the velocity of (5 m/s), the effectiveness only reaches a value of (32.82, 32.05, 30.45 %) for the same respective tilt angle. It is apparent from Figures (11), (12), and (13) for all bend angles that when water is injected towards the inner wall of the duct, i.e., the injection at a nozzle tilt angle of ( $\phi=-45^\circ$ ), the droplets will not benefit from the centrifugal forces due to the droplet drift outward and spread across the duct. However, they will collect through the separation zone, and thus the outer part of the duct becomes warmer, which affects the average temperature at the end of the duct. Nevertheless, the water injection in the direction of the outer wall will make the droplets rotate inside the vortex cells of the secondary flow and lead them to progress within the separation zone moderately. Hence, a better spread of droplets is evident, making most of the ducts at lower temperatures. The layer adjacent to the outer wall and slower flow will not adequately motivate a higher evaporation rate. This effect makes temperatures near the outer wall high until the duct's end, where the average temperature there is higher. The best case was observed when the water injection is in the axial direction at nozzle tilt angle ( $\phi=0^\circ$ ). The water droplets will be distributed in an orderly manner, and the contact area between the air and the water droplets will become enormous. The droplets will return to spread across the duct downstream of the bend due to fast entrainment with an airstream away from the separation zone. Therefore, the heat exchange will be better for the entire duct section, and the average temperature at the end of the duct is the lowest compared to the other nozzle tilt angles. Figure (14) shows the comparison between the cooling of air stream traveling through a straight duct with that traveling through a duct with a bend angle of ( $\lambda=135^\circ$ ) under the same operating condition. The figure clarifies the average temperature and relative humidity with bent duct over straight duct due to the generation of secondary flow, which helps more mixing between airflow and water droplet. The case of straight duct gives an average temperature of (90.40, 85.15, 76.15%) at air velocity of (5, 3.75, 2.5 m/s) with corresponding average relative humidity of (146.30, 182.06, 262.50%). However, the case ( $135^\circ$ ) bent duct achieves an improvement of about (8.24%) in temperature and (33.28%) in relative humidity over that of the straight duct at the best velocity of (2.5 m/s).

## 6. Conclusions

The resulting conclusions are drawn from the investigation of numerical analysis and experimental testing procedure in the present work:

- 1) Decreasing the air velocity from (5 to 2.5m/s) improves the cooling extent for all nozzle tilt angles at the three-bend angle due to the more time available for the droplets to exchange heat and mass with the airstream.
- 2) Injecting water towards the inner or the outer wall brings a lower cooling extent due to the poor mixing and evaporation of water droplets. This fact applies to all bend angles.
- 3) Axial water injection at 0° tilted injector provides the highest temperature reduction of the treated air for all bend angles and promises the optimum position of the water injectors.
- 4) The favorable bend geometry observed is when the curved duct has a 135° bend angle giving the utmost cooling of about 16% and excels the other angle of 45° and 90° of about 6% and 3%, respectively.
- 5) The humidification process through the bent duct is susceptible to the flow and mixing within the inner half of the duct due to the secondary flow at the separation zone.

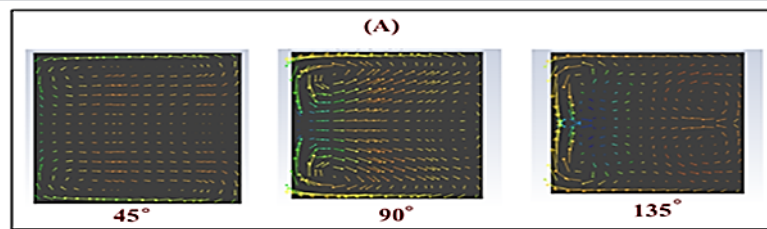


**Figure 7:** Flow structure downstream of different bend angle duct with air velocity of (A) V=2.5 m/s; (B) V=3.75 m/s; (C) V=5 m/s

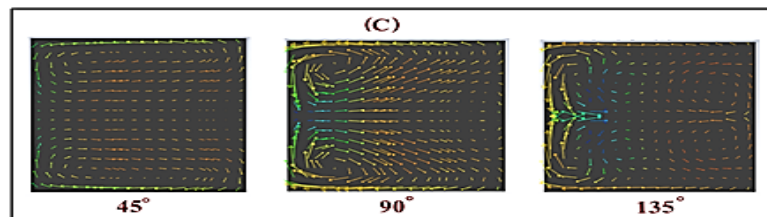
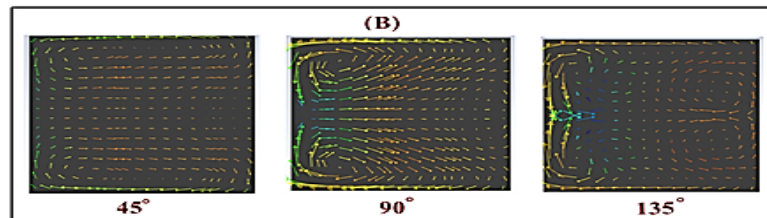


**Figure 7 Continued**

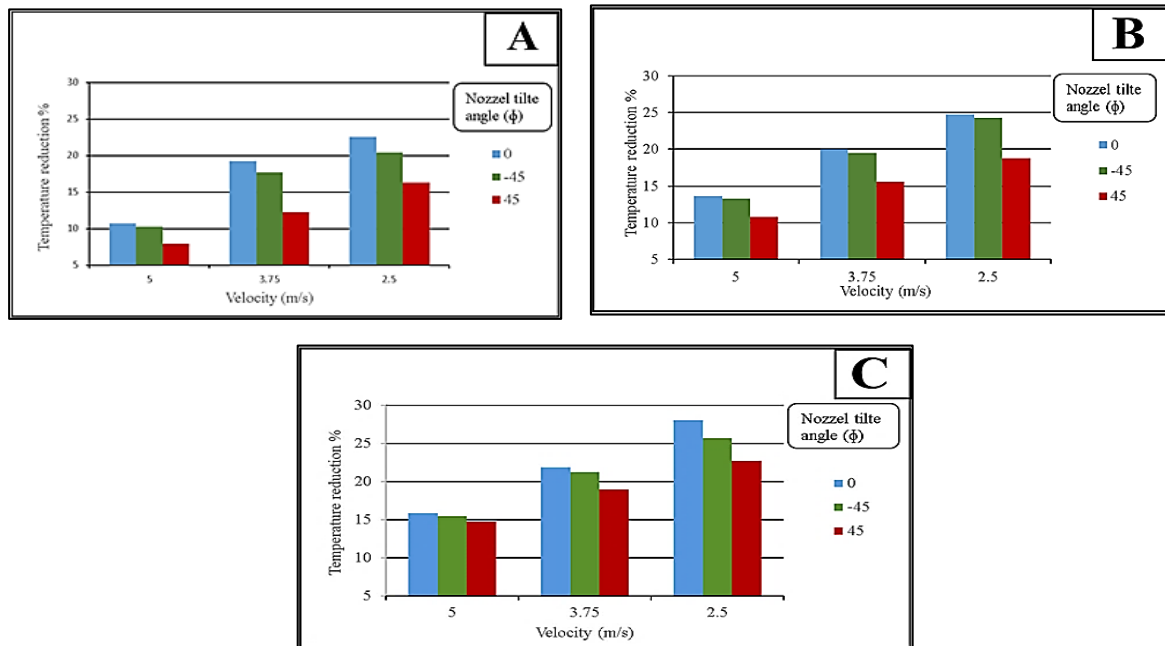


**Figure 8:** Effect of air velocity and nozzle tilt angle on Temperature reducton at (A) λ=45°; (B) λ= λ=90°; (C) λ= λ=135°



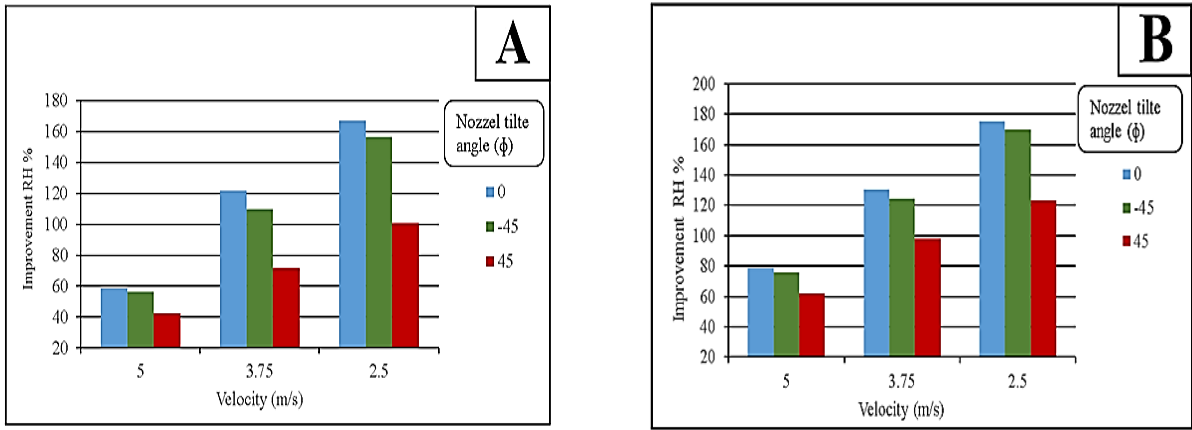


Figure 9: Effect of air velocity and nozzle tilt angle on improvement in relative humidity at (A)  $\lambda=45^\circ$ ; (B)  $\lambda= \lambda=90^\circ$ ; (C)  $\lambda= \lambda=135^\circ$

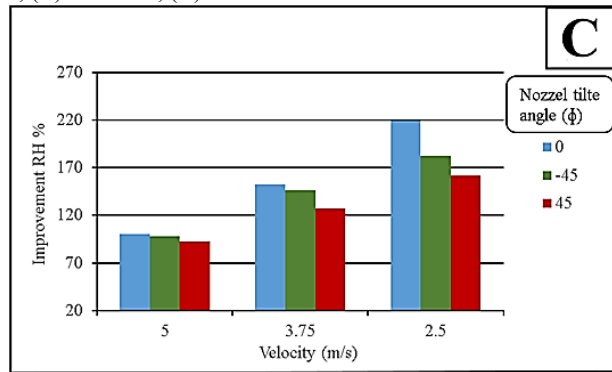


Figure 9 Continued

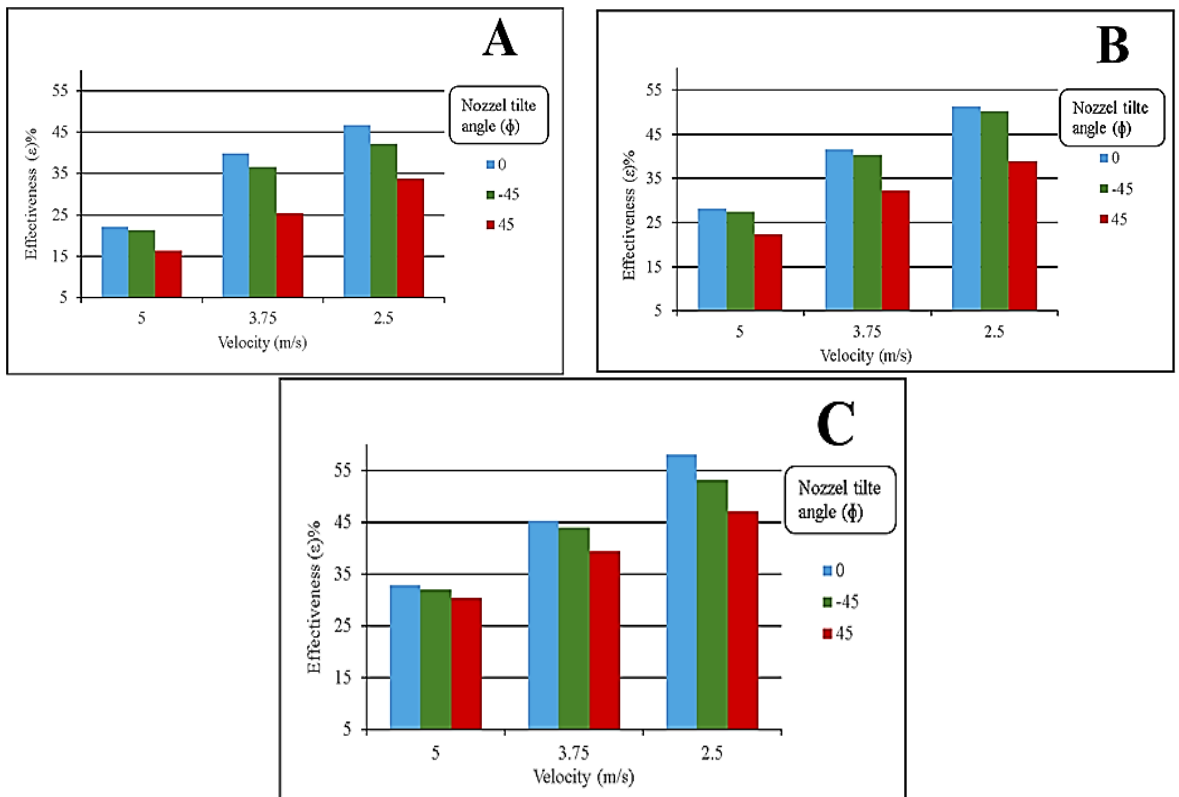


Figure 10: Effect of air velocity and nozzle tilt angle on the evaporative cooling effectiveness at (A)  $\lambda=45^\circ$ ; (B)  $\lambda= \lambda=90^\circ$ ; (C)  $\lambda= \lambda=135^\circ$

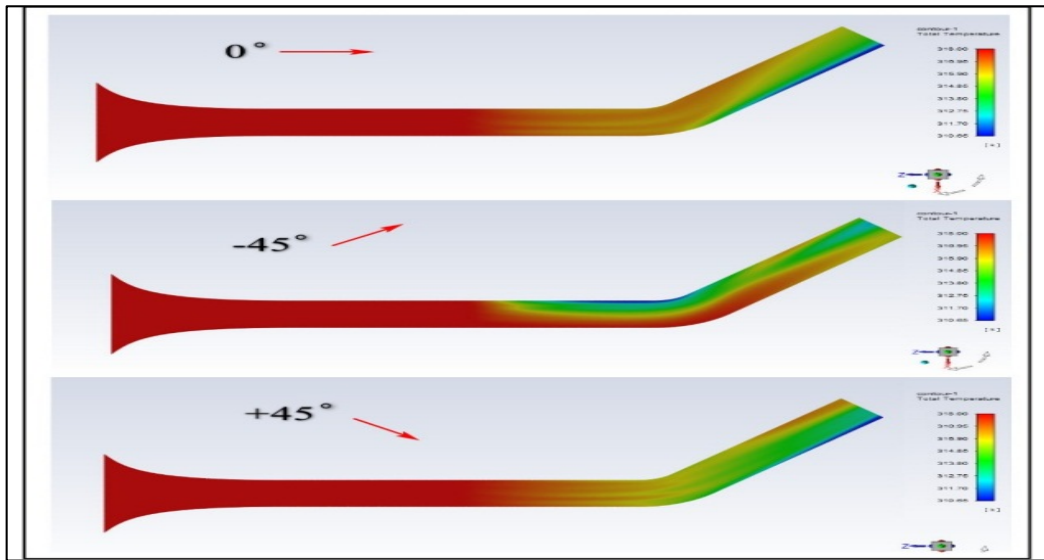


Figure 11: The effect of changing nozzles tilt angle on air temperature distribution in the (X-Z) planar (top view) for bend angle with  $\lambda=45^\circ$

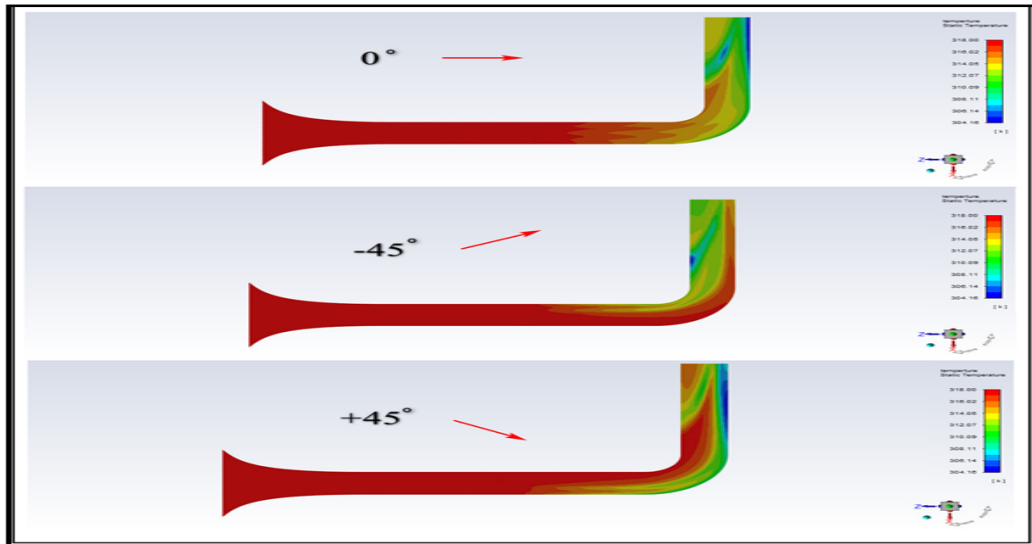


Figure 12: The effect of changing nozzles tilt angle on air temperature distribution in the (X-Z) planar (top view) for bend angle with  $\lambda=90^\circ$

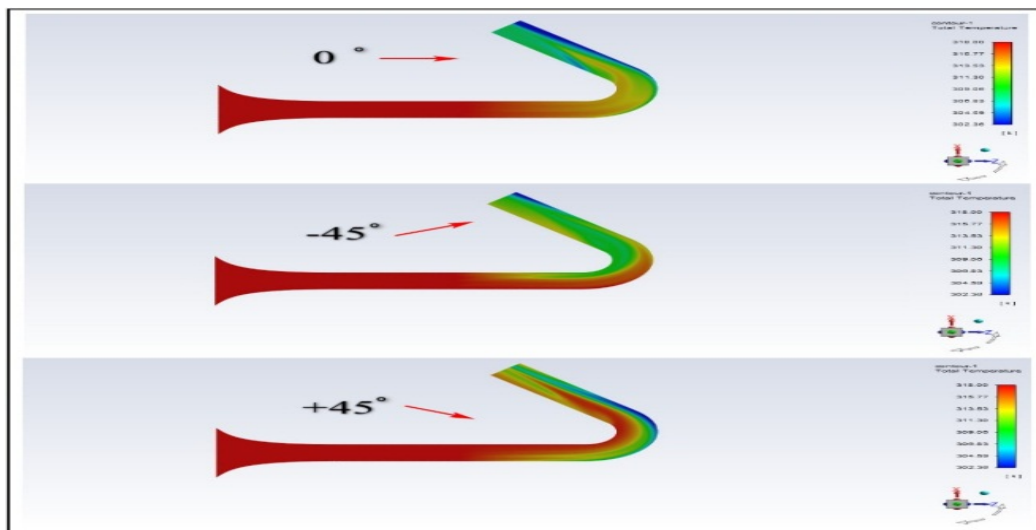


Figure 13: The effect of changing nozzles tilt angle on air temperature distribution in the (X-Z) planar (top view) for bend angle with  $\lambda=135^\circ$

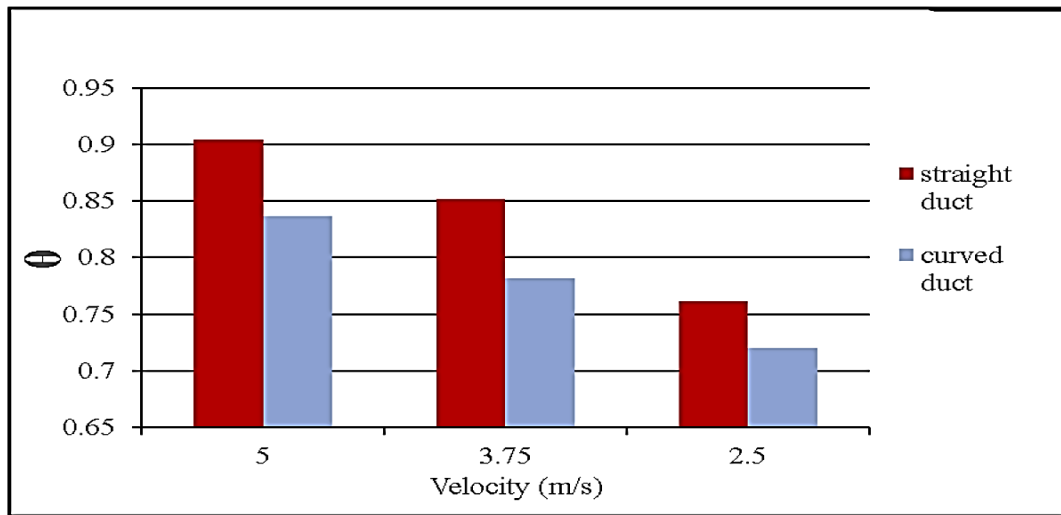


Figure 14: Comparison between straight duct and duct with (λ=135°) bend angle

**Nomenclature and units**

a	The duct width	m	Dimensionless parameters		
b	The duct height	m	Dn	Dean number	$Dn = Re \sqrt{D_h / \check{R}_c}$
D <sub>h</sub>	Hydraulic diameter	m	Re	Reynold number	$Re = u \cdot \rho \cdot D_h / \mu$
R <sub>c</sub>	bend Inner radius	m	β	Vertical probe	$\beta = Y_n / b$
$\check{R}_c$	Mean bent radius	m	ζ	Horizontal probe	$\zeta = X_n / a$
RH	Relative humidity	%	Θ	Temperature	$\Theta = T_n / T_{amb}$
T	temperature	°C	Ψ	Relative humidity	$\Psi = RH_n / RH_{amb}$
u	Velocity	m/s	Subscript		
Φ	Nozzle tilt angle	deg	amb	Ambient	
λ	Bend angle	deg	ave	Average	
ρ	Density	kg/m <sup>3</sup>	i	At any element	
μ	viscosity	Pa. s	n	At any location	
X	Horizontal location	cm	Abbreviations		
Y	Vertical location	cm	CFD	Computational fluid dynamics	
Z	Axial location	cm	R	Renormalization Group Analysis	
			NG		
φ	Nozzles tilt angles	deg			
λ	Bend angle	deg			
ρ	Density	kg/m <sup>3</sup>			

**Author contribution**

All authors contributed equally to this work.

**Funding**

This research received no specific grant from any funding agency in the public, commercial, or not-for-profit sectors.

**Data availability statement**

The data that support the findings of this study are available on request from the corresponding author.

**Conflicts of interest**

The authors declare that there is no conflict of interest.

## References

- [1] M. Boutabaa, L. Helin, G. Mompean, L. Thais, Numerical study of Dean vortices in developing Newtonian and viscoelastic flows through a curved duct of square cross-section Étude numérique des vortex de Dean de fluides Newtonien et viscoélastique en écoulement non établi dans une conduite courbe à section carrée, *Comptes. Rendus. Mécanique.*, 337 (2009) 40-47. <https://doi.org/10.1016/j.crme.2008.11.001>
- [2] A. S. J. Mohammed1 , S. G. Abed-Alfathel, the Effect of Curvature Ratio on Flow Structure and Fluids Mixing in 90o bent square duct, *J. Univ. Babylon Eng. Sci.* , 28 (2020) 144–159.
- [3] P. Dutta , N. Nandi, Numerical Study on Turbulent Separation Reattachment Flow in Pipe bends with Different Small Curvature Ratio, *J. Inst. Eng. India Ser., C* 100 (2019) 995–1004 . <https://doi.org/10.1007/s40032-018-0488-9>
- [4] S. Mondol, Md. Hossain, Md. Islam, Characteristics of Gas Flow through Bend Pipes of Different Angles IOSR, *J. Interdiscip. Math.*, 14 (2018) 85-93 .
- [5] M. Anwer, R. M. C. So, Y. G. Lai, Perturbation by and recovery from bend curvature of a fully developed turbulent pipe flow, *Phys. Fluids.*, (1989) 1387–1397. <https://doi.org/10.1063/1.857315>
- [6] Y. D. Tridimas, N. H. Woolley, A study of turbulent flows in pipe bends, *Proc .Inst. Mech. Eng .C .J. Mech. Eng .Sci .* , 204 (1990) 399–408 .
- [7] P. Dutta , N. Nandi, Effect of Reynolds number and curvature ratio on single phase turbulent flow in pipe bends, *Mech. Mech. Eng .* , 19 (2015) 5–16.
- [8] R. you, k. wei, Z. tao, h. li, G. xu, Development of secondary flow field under rotating conditions in a straight channel with square cross-section , *Chinese. J. Aeronaut.*, 31 (2018) 1703-1715 . <https://doi.org/10.1016/j.cja.2018.06.008>
- [9] S. K. Wang, *Handbook of Air Conditioning and Refrigeration*, the McGraw-Hill Companies, (2001).
- [10] R. Maurya, N. Shrivastava , V. Shrivastava, Performance Evaluation of Alternative Evaporative Cooling Media, *Int. j. sci. eng. res.*, 5 (2014) 676-684.
- [11] H. H. M. Ali, Abdul Satar. J. Mohammed, S.T. Ahmed., The Effect of Atomizer Position in a Curved Duct on the Humidification Process of Steadily Flowing Air, *Eng. Tech. J.*, 31 (2013) 793-815.
- [12] J. Mohammed, H. A. Nasser-allah, The Effect of Turbulences Flow on a Gas-Liquid Mixing Process Downstream of a Curved Duct, *J. Univ. Babylon. Eng. Sci.*, 26 (2018) 147-157.
- [13] A. S. J. Mohammed . S. G. Abed-Alfathel , The Effect of Curvature Ratio on Flow Structure and Fluids Mixing in 90o bent square duct, *J. Uni. Baby. Eng. Sci.*, 28 (2020).
- [14] ASHRAE, *HVAC Systems and Equipment, Handbook*, ASHRAE Inc., Atlanta; (2000).
- [15] B. ABRAMZON , W. SIRIGNANO, Droplet vaporization model for spray combustion calculations Modele de vaporisation de gouttelette pour les calculs de la combustion Ein tropfenverdampfungsmodell für die berechnung der verbrennung von brennstoffnebel, *Int. J. Heat. Mass. Transf.*, 32 (1989) 1605–1618. [https://doi.org/10.1016/0017-9310\(89\)90043-4](https://doi.org/10.1016/0017-9310(89)90043-4)
- [16] A. Collin, P. Boulet, G. Parent, D. Lacroix, Numerical simulation of a water spray—Radiation attenuation related to spray dynamics, *Int. J. Therm. Sci.*, 46 (2007) 856–868. <https://doi.org/10.1016/j.ijthermalsci.2006.11.005>
- [17] T. M. Soe, S. Yu. Khaing, Comparison of Turbulence Models for Computational Fluid Dynamics Simulation of Wind Flow on Cluster of Buildings in Mandalay, *Int. J. Sci. Res. Publ.*, 7 (2017) 337–350.
- [18] M. Cable, An Evaluation of Turbulence Models for the Numerical Study of Forced and Natural Convective Flow in Atria, *MSC. Thesis*, Queen's University, (2009).
- [19] N. Nivedita, P. Ligrani, I. Papautsky, Dean Flow Dynamics in Low-Aspect Ratio Spiral Microchannels, *Sci. Rep.*, 7 (2017) 44072. <https://doi.org/10.1038/srep44072>